

Development of Slotted Steel Shear Walls Capable of Detecting Damage States



T. Okamura

Taisei Corporation, Japan

M. Kurata & M. Nakashima

Disaster Prevention Research Institute, Kyoto University, Japan

15 WCEE

LISBOA 2012

SUMMARY:

A structural component capable of correlating its damage states with experienced deformation is beneficial as a passive damage indicator for visual inspection. A structural system developed with this new concept is a “steel shear wall with slits” which employs its out-of-plane deformation as an indicator of damage state. By inspecting residual buckling after an earthquake event, the maximum drift angle of the story that the shear wall is placed is estimated. This paper presents a series of experimental tests of the new shear wall conducted to validate the feasibility of the new concept.

Keywords: *Shear wall, Slit, Lateral Torsional buckling, Damage assessment*

1. INTRODUCTION

In an emergency situation when a large number of buildings in a densely populated urban area are subjected to strong earthquake ground motions, a damage-screening process must be rapid in order to allow each structure and/or community to regain functionality as quickly as possible. In Japan, the standardized campaign for quickly investigating safety risks in earthquake-damaged buildings was conducted for the first time following the Kobe Earthquake (1995), and since then the need of such investigations has continued to grow as witnessed in the Tohoku Earthquake (2011) [Kenchiku Bosai, 2011]. The Kobe earthquake was followed by an investigation of 46,610 buildings involving 6,468 registered investigators who were qualified with sufficient knowledge in structural engineering [Kenchiku Bosai., 2010]. The investigations require intensive labor, with investigators visiting each building on foot or by bicycle, and the required time for completing damage screening after a large earthquake in the Tokyo metropolitan area is estimated to be 6 months.

A damage assessment technology, which evaluates the structural integrity of buildings after major earthquakes, is beneficial in making prompt decisions on whether the buildings are operational or in need of actions for seismic retrofits. Structural health monitoring (SHM) and structural analysis using computer software are the examples of common technologies to evaluate the fragility of structures against earthquakes. In a SHM system, a dense array of sensors deployed to buildings measure structural response against ambient or earthquake loadings and damage state of structures are indirectly estimated from the collected data [*e.g.*, Aktan *et al.*, 1997; Sohn *et al.*, 2003]. However, cost and labor of sensor installation as well as the issues associated with long-term maintenance of sensors still hinder the true benefit of the SHM system to ordinary buildings.

On the other hand, adding a damage assessment feature to conventional passive energy dissipating devices is a feasible idea enabling quick inspection of building damage without the needs of installing expensive sensors. A slotted shear wall that has many vertical slits in a steel plate is an example of such devices (Fig. 1) [*e.g.*, Hitaka and Matsui, 2003; Hitaka *et al.*, 2007]. In the wall, each segment divided by two neighboring slits behaves as a flexural element, with its strength and stiffness controlled by the length and width of the segment. Deforming mainly in bending, these segments

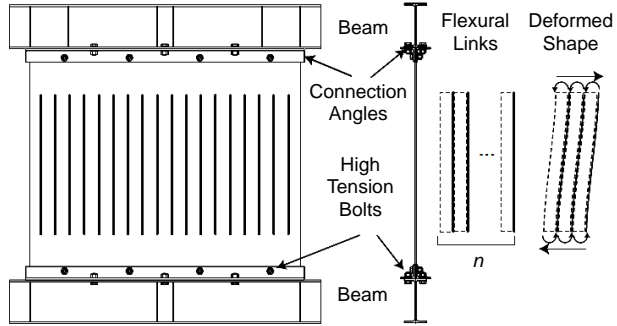


Figure 1. Slotted shear wall

show large deformation capacity without the need of adding out-of-plane strengthening and stiff boundary elements, which consequently enables the layout of placing the slotted shear wall in the middle of a beam span. Meanwhile, these segments buckle out-of-plane for large in-plane deformation. Since the in-plane deformation at the onset of out-of-plane buckling of segments can be controlled by the length and width of segments, it has strong potential as an indicator of the maximum in-plane shear drift that the wall has experienced.

This paper presents a new slotted shear wall specifically designed for a quick and simple approach for assessing the damage in buildings by adding explicit damage features to be evaluated by visual inspection. To explore the feasibility of this idea, slotted shear wall specimens designed with preliminary parametric analyses were tested under quasi-static cyclic loadings with various test parameters: the length and width of the segment, and loading history. In the test, the initiation of the lateral torsional buckling in each segment, the growth of out-of-plane deformations, and the magnitude of out-of-plane deformations in both the maximum and residual (corresponding to zero shear) wall drifts were carefully observed.

2. DAMAGE STATE ASSESSMENT BASED ON VISUAL INSPECTION

The idea for detecting damage state utilizes the out-of-plane deformation of a steel plate shear wall as an indicator of the maximum in-plane shear drift that the wall has experienced. This is achieved by the arrangement of many segments having a variety of widths in one shear wall. The segments sustain lateral torsional buckling when the wall sustains large in-plane shear drift, and its out-of-plane deformation, both maximum and residual, varies in accordance with the width of the segment. For smaller in-plane shear drift, a wider segment exhibits lateral torsional buckling and according out-of-plane deformations, while narrower segments sustain buckling and out-of-plane deformations for larger in-plane shear drifts. The segments once buckled sustain their deformed shape, and the number of buckled segments monotonically increases as in-plane shear drift increases. Thus, the maximum in-plane shear drift is evaluated by checking how narrow a segment is buckled. Here, a series of segments used for estimating the maximum in-plane shear drift are named “monitoring links”.

Three levels of damage state are suggested with respect to the in-plane shear drift R sustained by a shear wall, with the assumption that the in-plane shear drift of a shear wall is more or less equal to the drift of the story reinforced with the shear wall. The first is an elastic limit where main structural members remain elastic and R is taken as 0.5 %, the second is an immediate occupancy limit where a damaged structure is recoverable with minor retrofit and R is taken as 1.0 %; and the third is a safety limit where a severely damaged structure is not operational and R is taken as 2.0 %.

3. EXPERIMENTAL STUDY OF SLITTED SHEAR WALL WITH MONITORING LINK

3.1 Test Specimens

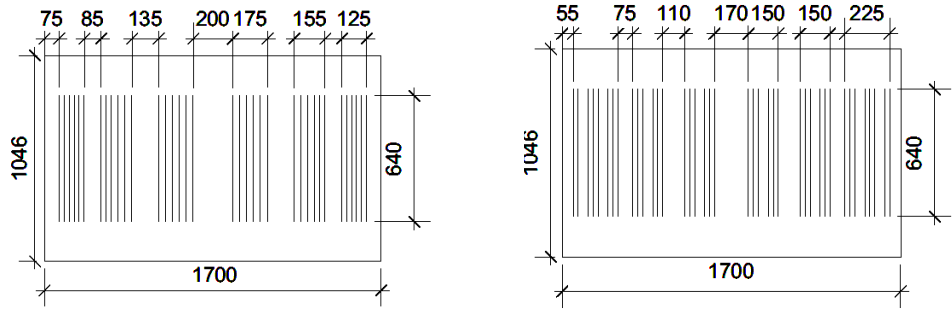


Figure 2. Details of specimens (Unit: mm): (a) specimen 1-3; (b) specimen 4

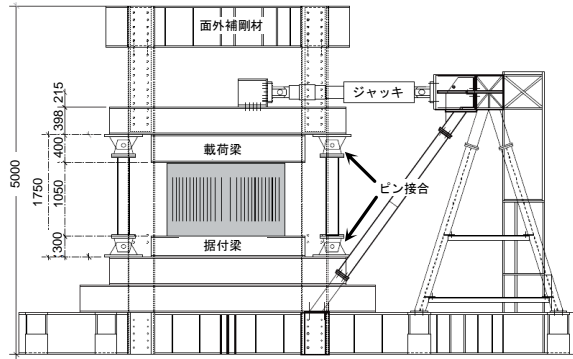


Figure 3. Test setup (Unit: mm)

To validate the idea on damage state assessment using a series of monitoring links, four slotted shear wall specimens were designed. All the specimens were made of 6 mm thick steel plate (SS400) and have the size of 1700 x 1046 mm. Three specimens (Specimens 1-3) have monitoring links of 200, 135, and 85 mm width (Figure 2(a)), while the other specimen (Specimen 4) has links of 170, 110 and 75 mm width (Figure 2(b)).

As shown in the figures, fine links with small width (named “cushioning link”) are inserted between the monitoring links. Jacobsen *et al.* have found such a cushioning link beneficial to prevent spreading of out-of-plane buckling from a wide monitoring link to an adjacent narrow monitoring link [Jacobsen *et al.*, 2010]. With the cushioning links, the monitoring links behave independently each other. The cushioning links in Specimens 1-3 have widths of 25 and 30 mm and those in Specimen 4 have widths of 25 and 50 mm.

3.2 Loading Protocol and Measurement Plan

Quasi-static loading tests were conducted at the structural laboratory in the Disaster Prevention Research Institute, Japan, using the test setup illustrated in Figure 3. The test setup was a pin-pinned steel frame consisted of wide-flange beams and columns; the top beam was restrained out-of-plane using steel restrainers. The specimens were connected to the boundary beams with four steel angles using slip-critical bolted connections. Installed at the top beam, a hydraulic jack with a maximum loading capacity of 1.5 MN force was used to apply the controlled displacement loading to the specimens.

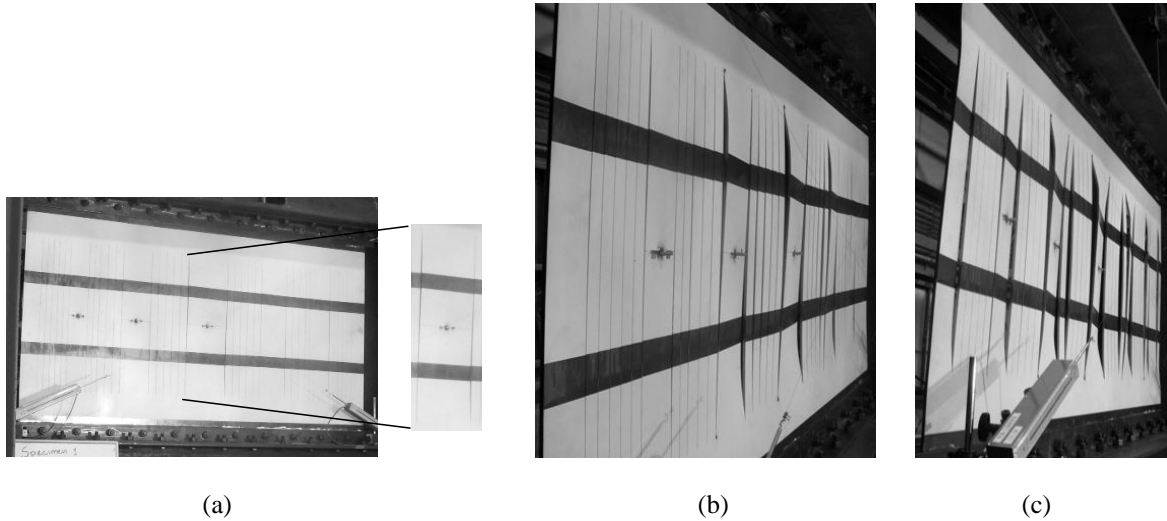
Table 1 shows the loading protocol used in the tests. Here, a wall drift R of 0.1 % corresponds to the expected elastic limit of the specimens. The Specimens 1 and 4 were subjected to normal incremental cyclic loadings. A larger number of loading cycles was assigned to Specimen 2 to examine the effect of the loading history on the out-of-plane buckling behavior of the monitoring links and to trace the strength deterioration under very large deformation of a wall drift of 4 %. Specimen

Table 1. Loading protocol

Wall drift R	Number of Cycles		
	Specimens 1, 4	Specimen 2	Specimen 3
0.1 %	2	4	2
0.5 %	2	4	2
0.1 %	-	-	2
1.0 %	2	4	2
0.5 %	-	-	2
1.5 %	2	4	2
1.0 %	-	-	2
2.0 %	2	4	2
1.5 %	-	-	2
3.0 %	2	4	2
4.0 %	2	10	2
6.0 %	1	1	1
8.0 %	1	1	1

Table 2. Expected behavior for out-of-plane buckling

Wall drift	Width of monitoring link	
	Specimens 1-3	Specimen 4
0.5 %	200 mm	170 mm
1.0 %	135 mm	110 mm
2.0 %	85 mm	75 mm

**Figure 4.** Test views of Specimen 1: (a) at the end of loading cycle for $R = 0.5\%$; (b) at the end of loading cycle for $R = 1.0\%$; (c) at the end of loading cycle for $R = 2.0\%$

2 experienced small loading cycles between large loading cycles to examine the influence of the non-stationary loading history commonly observed in real earthquakes. Table 2 summarizes the width of buckled monitoring link expected at different wall drifts.

In the tests, two Linear Variable Differential Transformers (LVDTs) were attached to the edges of each monitoring link at its middle height to monitor the out-of-plane rotation of the link. The link rotation angle φ obtained from the LVDTs and the wall drift at the onset of out-of-plane buckling R_{cr} , which was determined through visual inspections, were compared.

3.3 Test Observations

The general behavior observed for the loading of Specimen 1 was as follows: (1) At the 0.1 % loading cycle, the specimen remained elastic; (2) Figure 4(a) shows the behavior of the specimen after the $R = 0.5\%$ loading cycles and returned to $R = 0\%$. The widest link ($b = 200$ mm) in the middle of the

Table 3. Buckled wall drift visually identified in the tests

Link width	Wall drift			Link width	Wall drift
	Specimen 1	Specimen 2	Specimen 3		
200 mm	0.5 %	1.0 %	1.0 %	170 mm	0.5 %
135 mm	1.0 %	1.0 %	1.0 %	110 mm	1.0 %
85 mm	2.0 %	1.5 %	2.0 %	75 mm	2.0 %

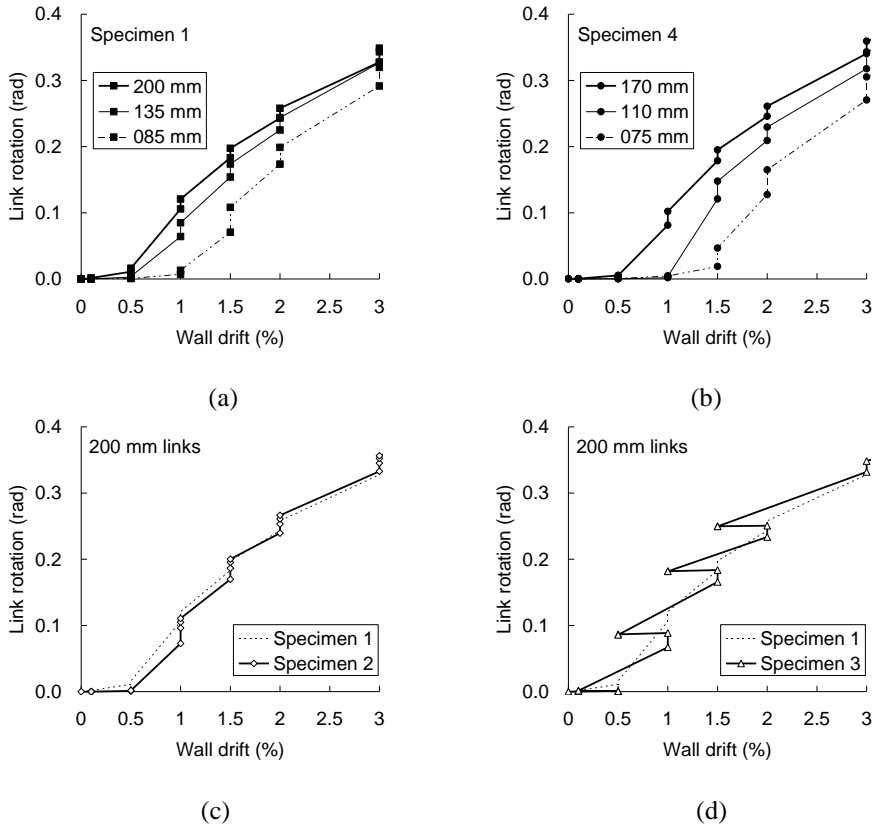


Figure 5. Link rotation angle φ : (a) Specimen 1; (b) Specimen 2; (c) Specimen 3; (d) Specimen 4

wall showed the out-of-plane buckling with its right-top edge deformed outwards and the left-bottom edge deformed inwards and the torsion angle of the entire link was around 0.016 rad; (3) Figure 4(b) shows the deformed behavior of the specimen at the end of loading cycles of $R = 1.0\%$ and retuned to $R = 0\%$ where, in addition to the widest link, the link with middle width ($b = 135\text{ mm}$) was also buckled; (4) The narrowest link ($b = 85\text{ mm}$) was buckled after loading cycles of $R = 2.0\%$ (Figure 4(c)). All the links were buckled at the expected wall drifts.

The out-of-buckling behaviors of all the specimens are summarized in Table 3. The expected behaviors were obtained in Specimens 1 and 4. In Specimen 2, the buckling of the widest link did not occur until the loading cycle of $R = 1\%$, which was later than expected, and the narrowest link buckled early at the 4th loading cycle of $R = 1.5\%$ mostly due to the large number of cyclic loadings. In Specimen 3, the widest link buckled at a slight delay at $R = 1\%$ wall drift. The reason of the delay of buckling relative to the prediction for the widest links in Specimens 2 and 3 were in part because of the initial stiffness K of these specimens, which were 20-25 % smaller than that of Specimen 1 (Table 4); the reason for stiffness reduction were under investigation.

Figure 5 shows the rotation angle of the monitoring links φ . The abscissa is the wall drift R and the ordinate is the link rotation angle φ measured at the end of each loading cycle. In Specimens 1 and 4, the buckling wall drift R_{cr} , which was visually determined, had a clear relationship with the link rotation angle φ for the monitoring links of widths of 200, 170, 135, and 110 mm. For example, the buckling wall drift R_{cr} was 0.5 % for the links of widths of 200 and 170 mm at which time the link started to rotate as well; the amount of the link rotations were $\varphi = 0.016\text{ rad}$ and 0.005 rad ,

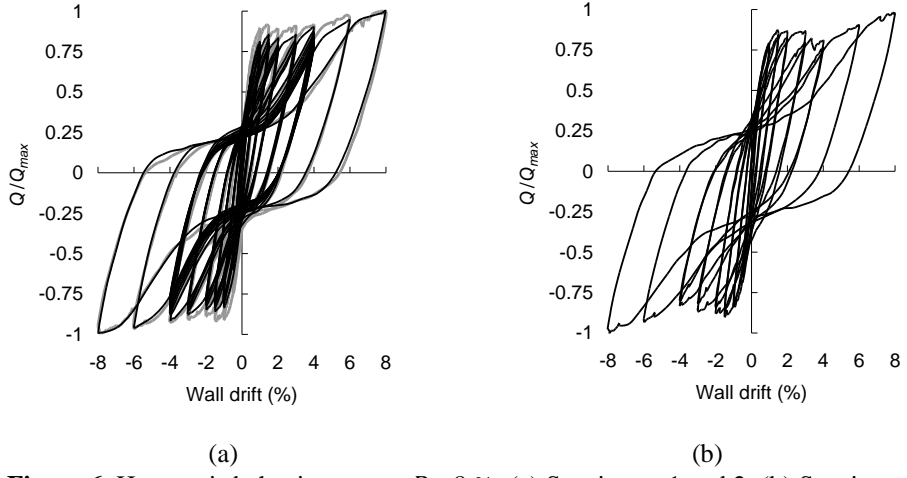


Figure 6. Hysteresis behaviour up to $R = 8\%$: (a) Specimens 1 and 2; (b) Specimen 4

Table 4. Summary of initial stiffness K , yield shear force Q_p and maximum shear force Q_{max}

	Specimen 1	Specimen 2	Specimen 3	Specimen 4
K (kN/mm)	26.4	19.0	18.4	20.6
Q_p (kN)	176.3	142.5	144.4	160.1
Q_{max} (kN)	192.4	166.9	168.8	177.8

respectively. However, the relation was not clear for monitoring links of widths of 85 and 75 mm. For example, the buckling wall drift R_{cr} was 2 % while the link started to rotate at a wall drift of $R = 1\%$; the amount of the link rotations were $\varphi = 0.013$ rad and 0.005 rad, respectively). The observation from experimental study revealed that, for a wall drift larger than $R = 1\%$, some links started to rotate in torsion prior to the onset of out-of-plane buckling. It was suggested that the onset of out-of-plane buckling should be identified by local dislocation of the steel plate at the top and bottom ends of the monitoring links.

The influence of the loading history was limited. Specimen 2, which was subjected to twice as many loading cycles, had a similar history for the link rotation angle. Specimen 3 showed that a loading with small amplitude after a loading with large amplitude had little effect on the link rotation angle.

3.4 Hysteresis Behavior

Figure 6 shows the hysteresis curves of Specimens 1, 2 and 4 in terms of normalized shear force and wall drift. In figure 6(a), the thick and thin lines correspond to Specimens 1 and 2, respectively. All the specimens reached yield shear force Q_p at a wall drift of $R = 1.5\%$; Table 4 summarizes the values of yield shear force. The strength of the specimens did not notably change until a wall drift of $R = 4\%$ and started to increase again with the development of a tension field in the monitoring links. The specimens showed the maximum shear force (Table 4) at a wall drift of $R = 8\%$.

4. CONCLUSIONS

This study presented a novel slotted shear wall capable of detecting damage states by visual inspection of its out-of-plane deformation. The presented damage detection approach was validated through a series of experiments. The main findings are as follows: (1) the residual deformations of the monitoring links were nearly as large as the maximum deformations meaning that the out-of-plane deformations were preserved once experienced; (2) the out-of-plane deformation of the monitoring links primarily depended on the maximum amplitude of the subjected shear loading and was not sensitive to small amplitude loading after the maximum drifts.

All of these findings encourage the use of the out-of-plane deformations in slotted shear walls as an indicator to estimate the experienced maximum shear drifts.

REFERENCES

- Abaqus Inc. (2007). ABAQUS Version 6.7 User's Manual, <http://www.abaqus.com>.
- Aktan, A.E., Farhey, D.N., Helmicki, A.J., Brown, D.L., Hunt, V.J., Lee, K.L. and Levi, A. (1997). Structural identification for condition assessment: experimental arts. *J. Struct. Eng. ASCE*. **123**, 1674 - 1684.
- Hitaka T., Matsui C. and Sakai J. (2007). Cyclic tests on steel and concrete-filled tube frames with Slit Walls. *Earthq. Eng. Struct. D.*, **36**, 707 - 727.
- Hitaka, T. and Matsui, C. (2003). Experimental study on steel shear wall with slits. *J. Struct. Eng.* **129**, 586 - 595.
- Jacobsen A., Okamura T. and Nakashima M. (2010). Performance of Unequally Slotted Steel Walls Under Large Lateral Drift Demands. Part 1: Condition Assessments through Strain Pattern Identification. *Summaries of Technical Papers of Annual Meeting AIJ*, Hokuriku, 1017 - 1018.
- KentickuBosai. (2010). Manual for Postearthquake Quick Inspection of Damaged Buildings. Japan Council for Quick Inspection of Earthquake Damaged Buildings. (a English manual is available from links in the following website: <http://www.kenchiku-bosai.or.jp/jimukyoku/Oukyu/oukyuindex/oukyuindex24.htm>).
- KentickuBosai. (2011). Japan Council for Quick Inspection of Earthquake Damaged Buildings, <http://www.kenchiku-bosai.or.jp/jimukyoku/Oukyu/Oukyu.htm> (in Japanese).
- Sohn, H., Farrar, C.R., Hemez, F.M., Shunk, D.D., Stinemates, D.W., Nadler, B.R. and Czarnecki, J.J. (2003). A review of structural health monitoring literature: 1996–2001., Cambridge: Los Alamos National Laboratory, USA.